Evaluation of the Virtual Crystal Approximation for Predicting Alloy Phonon Properties and Thermal Conductivity

Jason M. Larkin[1] and A. J. H. McGaughey[1,*]

[1]*Department of Mechanical Engineering*

Carnegie Mellon University

Pittsburgh, PA 15213

(Dated: March 13, 2013)

Abstract

The virtual crystal approximation for mass disorder is evaluated by examining two model alloy systems: Lennard-Jones argon and Stillinger-Weber silicon. In both cases the perfect crystal is alloyed with a heavier mass species up to equal concentration and phonon frequencies, lifetimes and group velocities and thermal conductivity are predicted. These two alloy systems have different ranges of phonon frequencies, lifetimes. For Stillinger-Weber silicon, the virtual crystal approximation predicts phonon properties and thermal conductivity in reasonably good agreement with molecular dynamics-based methods. For Lennard-Jones argon, the virtual crystal approximation underpredicts the high-frequency phonon lifetimes, leading to an underpredicting of its thermal conductivity. Resolution of this underprediction is achieved by considering methods that treat the disorder explicitly.

spelling! Fix before sending next version

Figures are nice

Work on figure captions

Parades End

Benedict C.

I. INTRODUCTION

Due to their low thermal conductivities, disordered materials (e.g., alloys, amorphous solids, aerogels) are used in applications ranging from thermoelectric energy conversion to thermally insulating barriers.[1-6] Disordered lattices are a subgroup of disordered materials where the atomic positions follow a lattice structure but the constituent species are spatially random. Examples include isotopic solids, where the species have the same electronic structure but small mass variations,[7,8] and alloys, our focus here, where two distinct species are present. (REF)

We further restrict our focus to dielectric or semiconducting solids, where the heat is conducted by the atomic vibrational modes. Predicting the thermal conductivity ~~of a dielectric or semiconducting solid~~ *such materials* requires the properties of the full spectrum of vibrational modes.[9-11] Accurate predictions of these ~~vibrational mode~~ properties for crystalline systems (i.e., perfect lattices) can be made with anharmonic lattice dynamics (ALD) theory using input from Denisty Functional Theory (DFT) calculations.[8,12-19] Computational costs limit DFT calculations to less than 100 atoms, however, making it challenging to explicitly incorporate the effects of disorder.[8,13,15,20-22]

~~For alloys (i.e., disordered lattices),~~ *D*isorder is typically included in the ALD framework using Abeles' virtual crystal (VC) approximation, whereby the disordered solid is replaced with a perfect VC with properties equivalent to an averaging over the disorder (e.g., atomic mass ~~and/or~~ bond strength).[23] The ALD calculations are performed on a small unit cell with the averaged properties (i.e., all vibrational modes are phonons) and phonon-phonon and phonon-disorder scattering are included as perturbations.[7,8,15,23] Except for low-frequency (long-wavelength) acoustic modes, the general validity of this assumption is unclear. We will refer to this approach as VC-ALD. Recent work using DFT calculations and the VC-ALD approach predicted relatively large ($\sim$ 10-100 W/m-K)[8,13,18] and small ($\sim$ 1 W/m-K)[15] *disordered lattice* ~~alloy~~ thermal conductivities that compared well with experimental measurements. No comprehensive study has been performed to assess the applicability of the VC-ALD approach for a range of disorder *strength*.

I thought there were no experiment

The objective of this study is to investigate the use of the VC approximation for predicting the vibrational mode properties and thermal conductivity of alloys by a detailed comparison of three predictive methods: (i) molecular dynamics (MD)-based normal mode decomposi-

2

tion (NMD), (ii) MD-based Green-Kubo (GK), and (iii) VC-ALD. By using computationally-inexpensive ~~cheap~~ empirical potentials for argon [Lennard-Jones (LJ)][24] and silicon [Stillinger-Weber (SW)],[25] we can self-consistently study the effects of disorder both explicitly and as a perturbation. For both materials, the perfect lattice is disordered with a heavier mass species up to equal concentration ~~(c = 0.5)~~, spanning a range of perturbative to large disorder. By spanning this range, the limits of the perturbative models are examined.

The remainder of the paper is organized as follows. In Section II, the theoretical formulation of thermal transport in ordered and disordered solids ~~is~~ and the computational framework are introduced. In Section III, the frequencies, group velocities, lifetimes, and thermal diffusivities of the vibrational modes of the LJ argon alloys are predicted when the disorder is explicitly modeled and when it is treated as a perturbation in the VC approximation. A breakdown of the VC-ALD method is identified by a comparison with the NMD method in Section III C 2 and a correction is suggested in Section III D. The vibrational mode properties are then used to predict thermal conductivities in Section IV, allowing for a comparison to the predictions of the top-down GK method, where no assumptions about the nature of the thermal transport are required. The vibrational mode properties and thermal conductivity of the SW silicon alloys are predicted ~~and~~ in Section V to provide a comparison and contrast to the LJ argon alloys, ~~which have different thermal conducitivity spectra than SW silicon alloys.~~ where low frequency modes dominate the thermal conductivity,

II. THEORETICAL AND ~~MODELING~~ Computational Frameworks ~~FORMULATION~~

A. Thermal Conductivity Prediction

To predict the thermal conducitivty of a disordered lattice, one begins with the theory for a perfect lattice. For a perfect lattice, all vibrational modes are phonon modes, which by defintion are delocalized, propagating plane waves.[9] Using the single-mode relaxation time approximation[9] to solve the Boltzmann transport equation[26] gives an expression for thermal conductivity in direction n [not italic]

$$k_{ph,\mathbf{n}} = \sum_{\kappa} \sum_{\nu} c_{ph}\binom{\kappa}{\nu} v_{g,\mathbf{n}}^2\binom{\kappa}{\nu} \tau\binom{\kappa}{\nu}. \tag{1}$$

Here, the sum is over the phonon modes in the first Brillouin zone, κ is the wave vector, and ν labels the polarization branch. The phonon mode has frequency $\omega\binom{\kappa}{\nu}$, volumetric specific heat $c_{ph}\binom{\kappa}{\nu}$, n-component of the group velocity vector $v_{g,\mathbf{n}}\binom{\kappa}{\nu}$, and lifetime $\tau\binom{\kappa}{\nu}$.

at a temperature of 300 K

at a Temperature of 10 K

B is not Italic in k_B

The relaxation time approximation has been found to be valid for lower thermal conductivity materials (e.g., Si and SiGe alloys),[12,13,27] while larger conductivity materials such as GaN and diamond require an iterative solution to the BTE for more accurate predictions.[8,28] For the crystalline LJ argon and SW silicon phases, the lattices and the components of their thermal conductivity tensors are cubically symmetric, so that we will refer to k_{ph} as an isotropic scalar thermal conductivity. This isotropy will hold for disordered lattices in the infinte size limit. Since MD simiulations are classical and obey Maxwell-Boltzmann statistics,[29] the volumetric specific heat is k_B/V per mode in the harmonic limit, where V is the system volume. This *harmonic* approximation has been shown to be valid for LJ argon and SW silicon at the temperatures of interest here[30] and is used so that direct comparisons can be made between the MD- and lattice dynamics-based methods.

For disordered systems, the vibrational modes are no longer pure plane-waves (i.e., phonon modes), except in the low-frequency (long-wavelength) limit. *When applied* In the classical limit, the Allen-Feldman (AF) theory computes the contribution of diffusive, non-propagating modes (i.e., diffusons) to thermal conductivity from[31]

$$k_{AF} = \sum_{diffusons} \frac{k_B}{V} D_{AF,i}(\omega_i), \qquad (2)$$

where $D_{AF,i}$ is the mode thermal diffusivity and ω_i is the frequency of the ith diffuson. The thermal diffusivity of diffusons can be calculated from harmonic lattice dynamics theory.[10,31,32] Assuming that all vibrational modes *travel with the sound speed (v_s) and* scatter over a distance of the lattice *constant, a,* ~~spacing~~, a high-scatter (HS) limit of thermal conductivity in the classical limit is[1]

$$k_{HS} = \frac{k_B}{V_b} b v_s a, \qquad (3)$$

where V_b is the volume of the unit cell, ~~v_s is the branch-averaged sound speed,~~ *and* b is the number of atoms in the unit cell ~~and a is the lattice constant~~. The HS limit will be used to discuss the differences between the LJ argon and SW silicon alloys.

B. Virtual Crystal Approximation

Under the VC approximation, the disordered solid is replaced with a perfect, single-species crystal with properties ~~such as~~ density *(ea.)*, ~~and and~~ cohesive energy equivalent to an averaging over the disorder (e.g., atomic mass ~~and/or~~ bond strength).[23] The VC approximation is

4

visualized for an alloy in Figs. 1(a) and (b), where an explicitly mass-disordered supercell is replaced by a perfect crystal with an averaged mass. Abeles first introduced the concept of a VC to predict the thermal conductivity of SiGe, (Ga,In)As and In(As,P) alloys, using Klemens-Callaway theory to model the phonon-phonon and phonon-defect scattering.[33-35] The Abeles theory is conceptually simple, treating both disorder and anharmonicity as perturbations, and leads to a closed-form analytical function for the thermal conductivity.[23] With the use of phenomenological fitting parameters, good agreement between the predictions and experimental measurements was found for SiGe and (Ga,In)As alloys. Deviations from the Abeles theory were observed for In(As,P) alloys at large concentrations of InP, which were attributed to the high mass ratio of 3.7 between In and P.[23]

The Abeles theory was developed using the VC approximation and Klemens-Callaway theory, which is valid for low-frequency modes and small perturbative disorder.[23,33-37] The application of the Abeles theory leads to good agreement between some experimental and computational results. When considering alloys, it is important to note that the overall disorder strength is determined by the mass ratio, the stiffness ratio, and the alloy concentration. Cahill and co-workers found that the thermal conductivity reduction in dilute Ge-doped Si epitaxial layers can be explained by mass perturbative disorder alone.[38,39] For example, as little as 6.2×10^{19} cm^{-3} Ge reduces the thermal conductivity of Si (mass ratio of 2.6) by a factor of two.[38] The relative effects of bond and mass disorder was investigated computationally using MD simulations by Skye and Schelling for SiGe up to equal concentration,[40] who also found that mass disorder is the dominant scattering mechanism.

Unlike the phenomenological Abeles theory, the VC-ALD approach predicts thermal conductivity by directly summing over the modes of the full vibrational spectrum, with phonon-phonon and phonon-defect scattering treated as perturbations.[8,13,15] In the VC-ALD method, the phonon-phonon scattering is predicted using ALD, which is a perturbative method that recovers the Klemens-Callaway theory predictions in the low-frequency, low-temperature limit. The phonon-defect scattering is treated using perturbative methods which can treat mass and/or bond disorder and recover the Klemens theory predictions at low-frequencies.[7,36] In the case of Ni$_{0.55}$Pd$_{0.45}$, which has a large mass ratio (1.8) and concentration of each species, experimental measurements of vibrational frequencies and linewidths agree well with predictions made by perturbative mass-disorder predictions.[36,37]

Using DFT methods to predict the mode-specific phonon properties of the VC, Lindsay

[handwritten: provide the isotope f_0 and mass ratio]

[handwritten: al measurements of thermal conductivity]

and Brido found good agreement between VC-ALD and experiment for isotopically defected GaN, ~~which has relatively small mass ratio of the isotopes.~~[8] Garg *[et al.]* used DFT calculations *[handwritten: what temperature?]* with VC-ALD to predict the thermal conductivity of SiGe alloys for all concentrations, obtaining good agreement with experiment.[13] Isotopically-defected GaN and low concentration SiGe alloys have relatively large thermal conductivities *at temperature of* 300 K (~ 100 W/m-K). Li et al used DFT calcualtions with VC-ALD to predict the thermal conductivity of $Mg_2Si_xSn_{1-x}$ (~ 10 W/m-K) in good agreement with experimetal measurements for all concentraitons.[18] *[handwritten: needed? breaks flow — not clear what the relevance is]*

The VC-ALD approach has also been used to predict the phonon lifetimes and mean free paths in GaAs/AlAs superlattices, but thermal conductivity predictions were not compared with experimental measurements.[19] Given all these results, 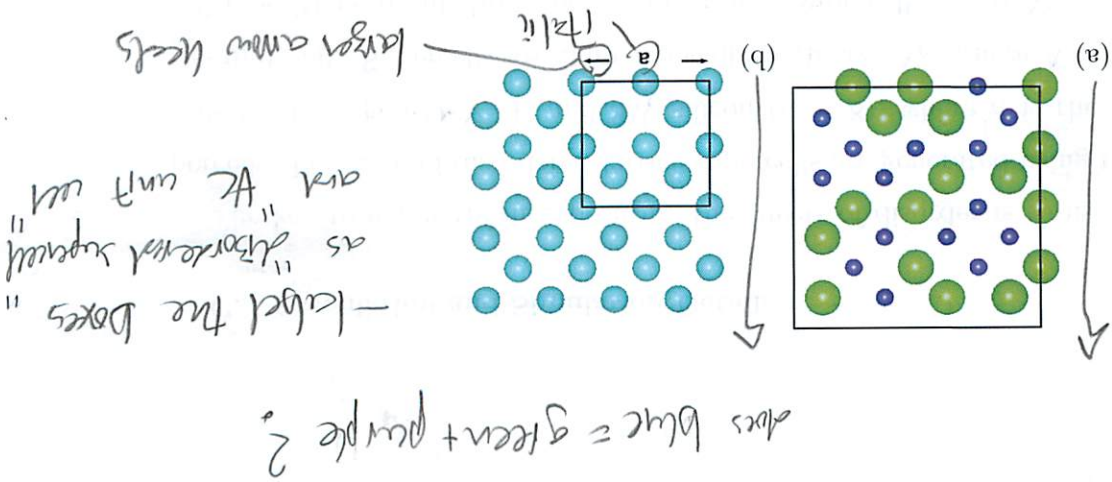it is unclear what limitations exist using the VC approach. ~~In our survey of~~ experimental mesurement and numerical modeling, we find that VC predictions tend to be accurate when the disordered lattice thermal conductivity is significantly above the high-scatter limit [Eq. (3)].[1,8,13,23,37-39] *[handwritten: which tends to be around 1 W/mK]*

An ALD study using phonon properties from DFT calculations for crystalline PbTe[14] predicted thermal conductivities (~ 1 W/m-K) for the perfect systems in fair agreement with experiment. For PbTe and PbSe alloys, a VC-ALD study predicted a small thermal conductivity reduction *[handwritten: compared to the perfect crystals]* with increasing concentration.[15] Experimental results lack for the alloys,[41,42] making it difficult to asses the validity of the VC-ALD approach for ~~these~~ materials whose thermal conductivities approach the ~~high scatter~~ *[handwritten: HS]* limit.[43]

In this study, we will consider a low thermal conductivity alloy using the LJ potential and a high thermal conductivity alloy using the SW potential. The computational studies discussed above were limited to VC-ALD because of DFT calcualtion costs. Our use of computationally ~~cheap~~ *[handwritten: inexpensive]* empirical potentials ~~will~~ allow us to include the disorder explicitly and as a perturbation and to compare the predictions.

[handwritten: ambiguous- PbTeSe alloy?]

FIG. 1: (a) view of an explicitly disordered supercell of Si and "heavy" Si ([100] direction into the paper). (b) view of the equivalent VC supercell with an average mass of the explicitly disordered Si and "heavy" Si supercell (b): Sphere size represents increasing mass only, no bond disorder is considered. In this work, calculations for LJ Ar and SW Si which use the VC approximation are based off of the conventional cubic unit cells (Section II G)

(handwritten annotations):

does blue = green + purple?

— label the Boxes,
"disordered supercell"
as
are "VC unit cell"

larger arrow heads

(121)

8-atom

is Shown in (b)

C. Calculation and Simulation Details

The key to explicitly incorporating the effects of disorder is to use large disordered supercells. Perfect and disordered lattice supercells are generated using the conventional unit cells for LJ argon ($n = 4$) and SW silicon ($n = 8$), where n is the number of atoms in the unit cell. Supercells are built cubically with size N_0, where N_0 is the number of unit cell repetitions in all three spatial directions. Supercells up to $N_0 = 12$ (6,096 atoms) are used for the LJ argon calculations. For SW silicon, $N_0 = 8$ (4,096 atoms) is used for the MD-based NMD calculations and $N_0 \leq 42$ (592,704 atoms) is used for the MD-based GK and VC-ALD.

Disorder is created by randomly specifying the masses of the atoms on the lattice. The composition of each lattice is labeled by $m_{1-c}^i m_c^j$, where (i) $m^i = 1$ and $m^j = 3$ in LJ units for argon, and (ii) $m^i = m_{Si}$ and $m^j = 2.6 m_{Si}$ for SW silicon and "heavy silicon", which has the mass of germanium. Concentrations, c, of $0.0, 0.05, 0.15$ and 0.5 are considered. Based on the previous works of others, we only consider mass disorder.

For LJ argon, the lattice constant at a temperature of 10 K is $5.290 Å$.[45] An amorphous LJ phase, discussed in Section III D, was created by liquifying the crystal and instantly quenching by removing all kinetic energy. The energy of the resulting structure was minimized and then annealed in an NPT (constant number of atoms N, pressure P, and temperature T) ensemble at zero pressure and a temperature of 10 K. The effective zero-pressure lattice constant of the amorphous phase at this temperature, based on the atomic density, is $5.389 Å$.[45] For SW silicon, the lattice constant is $5.43 Å$ for all calculations, which brings the GK thermal conductivty predictions at a temperature of 300K[46,47] into agreement with VC-ALD predictions.[48]

The MD simulations were performed using LAMMPS.[49] All MD simulations are first equilibrated in a NVT (constant number of atoms, volume, and temperature) ensemble for 10^6 time steps. Data is then collected from simulations in the NVE (constant number of atoms, volume, and total energy) ensemble. For LJ argon, the potential energy is cutoff and shifted at $8.5 Å$ (the force is not adjusted). Time steps of 4.285 and 0.5 fs were used for the LJ argon and SW silicon simulations. The same atomic trajectories are used for the NMD and GK methods.

The methods used in this work scale differently with the size of the supercell. The

This paragraph still feels like baggage — try to smooth it out, more details are OK

(random comments)

calculations ~~in this work~~ are trivially parallelizable except the MD simulations[49] and the eigenvalue solution of the dynamical matrix.[50] Efficient MD codes *like LAMMPS* scale linearly with the number of atoms in the system, N_a. The Gamma-NMD and AF theory require the eigenvalue solution of a large dynamical matrix of size $(3N_a)^2$ that scales as $[(3N_a)^2]^3$ and ~~limits the~~ system sizes considered.[50]

[Maybe include these details when you first discuss the techniques? MD - here NMD - next section AF]*

III. VIBRATIONAL MODE PROPERTIES IN ALLOYS

write out abbreviations here

NMD - III C 1
AF

A. VC and Gamma DOS

discuss computational costs here?

In this section, we begin to examine the effects of explicitly including disorder by computing the frequencies and density of states (DOS) for *the* vibrational modes of disordered LJ lattice supercells and their equivalent VCs. The frequencies are computed using harmonic lattice dynamics calculations with GULP.[50] For the VC, the allowed wave vectors are set by N_0 and due to the use of the conventional unit cell, there are 12 polarization branches per wave vector. For the disordered supercells, the only allowed wave vector is the gamma-point (i.e., $\kappa = 0$) where there are $12N_0^3$ polarization branches.

The DOS for the VC and the explicitly-disordered supercells (referred to herein as Gamma) are plotted in Figs. 2(a), 2(b), and 2(c) for concentrations of 0.05, 0.15 and 0.5 for $N_0 = 12$ (6,912 atoms). The VC and Gamma DOS agree at low frequencies for all concentrations, where they follow the prediction of the Debye approximation that *the DOS will scale as* ~~the~~ ω^2.[24] Similar agreement between VC and Gamma *DOS* at low frequencies was found in DFT predictions for Si_cGe_{1-c}[13] and classical models of amorphous Si_cGe_{1-c}.[51] The Debye approximation underpredicts the DOS at moderate frequency, which is due to non-linearities in the dispersion, *but the VC and Gamma predictions remain in good agreement.*[24]

The increasing average atomic mass with increasing concentration for the VC shifts all frequencies downward by a factor $1/[(1-c)m^i + cm^j]^{1/2}$. The increasing average atomic mass for the Gamma modes also reduces the frequencies, but not in a systematic manner. The effect of the disorder is seen at ~~high~~ frequencies greater than ten by a broadening and *a* shift of the Gamma DOS to higher frequencies because of the explicit use of light atoms in the supercell. This effect becomes more pronounced as the concentraiton increases. Duda et al. observed similar high-frequency broadening effects in model LJ alloys ~~from MD simulation~~.[52]
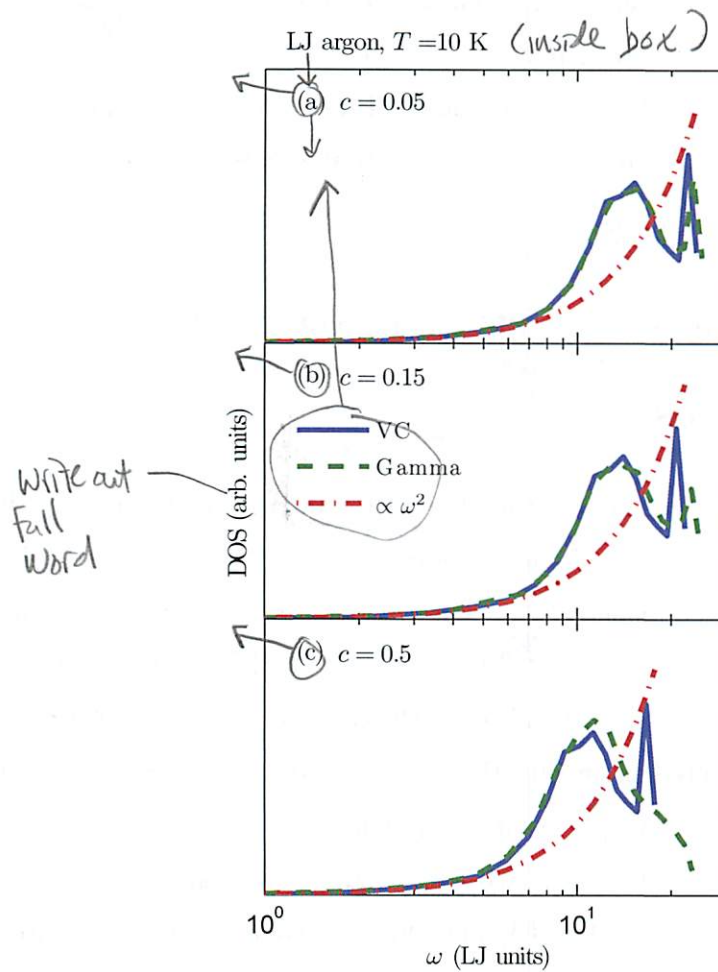
9

LJ argon, $T = 10$ K (inside box)

FIG. 2: Density of states (DOS) for modes calculated using the LJ FCC VC versus an explcitily mass disordered LJ FCC supercell (labeled Gamma) with varying mass concentration c. VC and Gamma show similar low-frequency behavior for all c. For increasing c, the frequencies of both VC and Gamma decrease, while the high frequency DOS for Gamma spreads and reaches up to a higher maximum frequency because of the explict disorder. The size of these supercells is $N_0 = 12$ (see Section II C).

[Handwritten annotations: "Vibrational" (above "Density"), "for LJ alloys" (above "calculated"), "approximately and" (above "explcitily"), "for" (above "with"), "concentrations" / "concentrations" (below "mass concentration"), "of (a) 0.05, (b) 0.15, and (c) 0.5." (right margin), "(___ atoms)." (right of $N_0 = 12$), "are of size" (below "supercells"), "Write out full word" (left margin), "are of size"]

Based on the DOS, the vibrational modes of the explicitly disordered supercells at low frequencies are phonon-like, while the broadening of the DOS at high-frequency indicates that the Gamma vibrational modes may differ from the VC phonon modes in this regime. This behavior is further investigated in the next three sections.

10

B. Dispersion and Group Velocity

The group velocity vector in a VC is defined as the gradient of the dispersion curve,

$$v_{g,n}\binom{\kappa}{\nu} = \frac{\partial \omega\binom{\kappa}{\nu}}{\partial \kappa}. \tag{4}$$

We calculate the group velocities for the VC using finite differences on the frequencies calculated from harmonic lattice dynamics.[53]

For a disordered solid, the three acoustic group velocities (two transverse and one longitudinal) can be predicted using the elastic constants[50] or by finite differencing of the three lowest frequency branches of the dispersion relation of a ~~a~~ *the* supercell.[54,55] Except for this low-frequency behavior, there is not an accepted method to predict the group velocity of a vibrational mode in a disordered system, although there have been attempts.[1,52,54–56] In the Cahill-Pohl (CP) model, for example, the group velocity of all disordered modes is the sound speed, v_s, which is also assumed for the ~~high-scatter~~ *HS* model, Eq. (3).[1] However, this is not a good ~~assumption~~ for any material, even in the amorphous phase.[32,52,54–56]

I think ← *cf distinguishes longs, trans.* *assumption* *what is the point of this comment?*

Calculating the structure factors of the supercell Gamma modes is a method to test for their plane-wave character at a particular wave vector and polarization corresponding to the VC.[11,32] Feldman et al. used the structure factor to predict an effective dispersion for a model of amorphous silicon, but did not predict group velocities.[32] Volz and Chen used the dynamic structure factor to predict the dispersion of crystalline SW silicon using MD simulation.[57]

The structure factor at a virtual crystal wave vector $\binom{\kappa_{VC}}{\nu}$ is defined as[11]

$$S^{L,T}\binom{\kappa_{VC}}{\omega} = \sum_\nu E^{L,T}\binom{\kappa_{VC}}{\nu}\,\delta\left[\omega - \omega\binom{\kappa=0}{\nu}\right], \tag{5}$$

where the summation is over the Gamma modes, ~~and~~ E^T refers to the transverse polarization and is defined as   *define = ℓ, α*

$$E^L\binom{\kappa_{VC}}{\nu} = \left|\sum_b \hat{\kappa}_{VC} \cdot e\binom{\kappa=0\ b}{\nu\ \alpha}\exp[i\kappa_{VC} \cdot r_0\binom{l=0}{b})]\right|^2 \tag{6}$$

and E^L refers to the logitudinal polarization and is defined as

$$E^T\binom{\kappa_{VC}}{\nu} = \left|\sum_b \hat{\kappa}_{VC} \times e\binom{\kappa=0\ b}{\nu\ \alpha}\exp[i\kappa_{VC} \cdot r_0\binom{l=0}{b})]\right|^2 . \tag{7}$$

In Eqs (6) and (7),
~~where~~ the summations are over the atoms in the disordered supercell, $r_0\binom{l=0}{b}$ refers to the equilibrium atomic positions of ~~the mass-disordered~~ atoms in the supercell, $\hat{\kappa}_{VC}$ is a unit   *and*

vector. Explicit disorder is also included ~~for~~ in the Gamma ~~mode~~ frequencies $\omega\binom{\kappa=0}{\nu}$ and eigenvectors $e\binom{\kappa=0\ b}{\nu\ \alpha}$, which have length $3N_a$. [handwritten: Not correct — $e\binom{\vec{\kappa}=0\ b}{\nu\ \alpha}$ is a scalar! is $\vec{e}\binom{\kappa}{\nu}$] [handwritten: The eigenvector]

Physically, $S^{L,T}\binom{\kappa}{\omega}$ represents the frequency spectrum required to create a wavepacket with a well-defined wave vector and polarization.[11,32,58] For a perfect lattice, the structrue factor peaks are delta functions centered at the mode frequencies, indicating that the modes are pure plane-waves (i.e., phonons). A sampling of the structure factors for the LJ argon

[handwritten left margin: (footnote 2, works well here)]

~~alloys are~~ plotted in Fig. 3 for wave vectors along the [100] and [111] directions in the $N_0 = 10$ systems. [handwritten: For these finite-size systems], the delta function in Eq. (5) is broadened using a Lorentzian function with a full-width at half maximum set to $20\delta_{\omega,avg}$, where $\delta_{\omega,avg}$ is the average frequency spacing.[32] Well-defined peaks at all wave vectors are due to the lattice structure of the disordered systems. Typically, the structure factor for amorphous materials has well-defined peaks only for small wave vector.[11,32] With increasing disorder, the structure factor spreads in width, particularly at high frequencies, which is an indication that the modes are not pure plane waves.

From Fig. 3, an effective dispersion curve (middle panel) can be extracted by locating the peaks in the structure factors at neighboring VC wave vectors. The peaks in the structure factor are larger than the VC predicted frequencies (plotted as solid lines in Fig. 3) by at most 5%. Similar agreement is found with the disordered SW silicon lattice supercells ~~(not shown)~~.

Because of the good agreement between the VC-predicted dispersion curves and the peaks in the structure factors from Fig. 3, we will use the group velocities predicted by the VC dispersion for both LJ argon and SW silicon with the VC-NMD and VC-ALD calculations for consistency and simplicity. We will [handwritten: discuss] ~~examine~~ the validity of this group velocity choice in Section III D.

[handwritten: — They agree well here, but later we argue for issues at high frequency — how to be consistent?]

12

13

ω(q,n) →

a/q,n →

S_L $\kappa\ (2\pi/N_0 a)$ S_T

10^4 1 2 3 4 5 10^2

10^2 10^4

ω (LJ units)

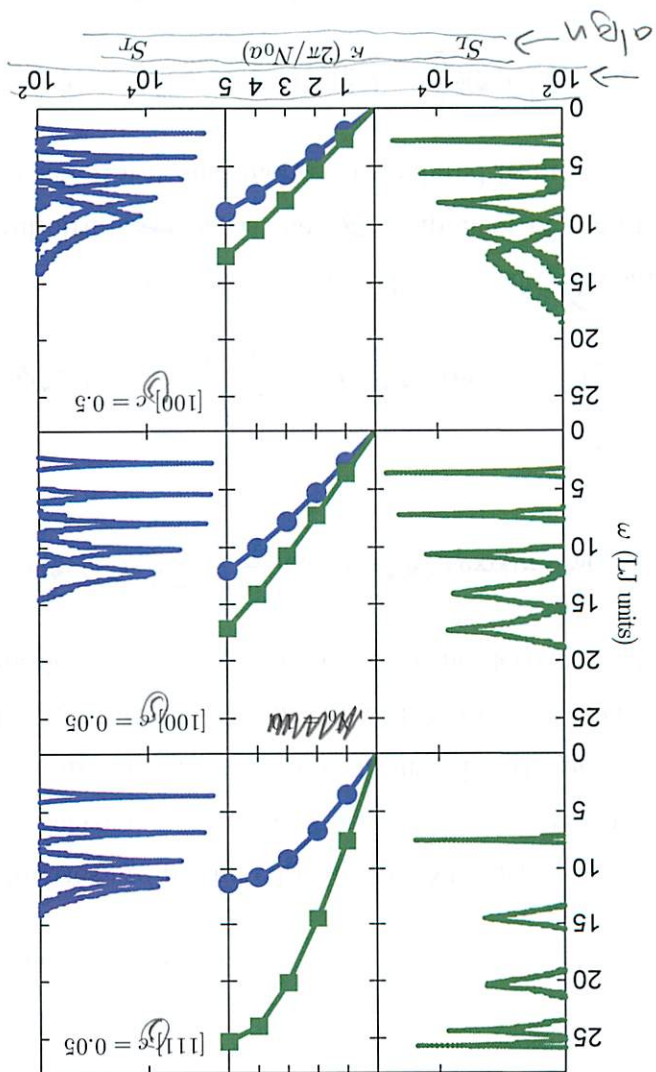[100] c = 0.5

[100] c = 0.05

[111] c = 0.05

FIG. 3: Left and Right Panels: The structure factor for longitudinal (S_L) and transverse (S_T) polarizations along high-symmetry directions ([100], [110]) where $\kappa = \pi/a$[100] and a is the lattice constant) of the mass disordered LJ argon supercells ($N_0 = 10, c = 0.05, 0.5$). For increasing mass disorder c, there is a decrease in the center of the peaks and an increase in the peak linewidths. Center Panel: The VC predicted dispersion at the same wavevectors used to calculate $S_{L,T}$.

curves (solid lines) agree well with the peaks in S_L and S_T.

measure the size of the pitch a LJ?

C. Lifetimes

1. From VC-NMD and Gamma-NMD

Once the group velocities are predicted using the VC dispersion, the mode lifetimes are required to predict the thermal conductivity using Eq. (1). As an alternative to the VC-ALD approach for predicting lifetimes, which is discussed in the next section, we first use the MD simulation-based NMD method.[59,60] In NMD, the atomic trajectories are first mapped onto the vibrational mode coordinate $q(\substack{\kappa \\ \nu}; t)$ and its time derivative $\dot{q}(\substack{\kappa \\ \nu}; t)$,[61]

$$q(\substack{\kappa \\ \nu}; t) = \sum_{\alpha,b,l}^{3,n,N} \sqrt{\frac{m_b}{N}} u_\alpha(\substack{l \\ b}; t)\, e^*(\substack{\kappa \ b \\ \nu \ \alpha}) \exp[i\kappa \cdot r_0(\substack{l \\ 0})] \tag{8}$$

and

$$\dot{q}(\substack{\kappa \\ \nu}; t) = \sum_{\alpha,b,l}^{3,n,N} \sqrt{\frac{m_b}{N}} \dot{u}_\alpha(\substack{l \\ b}; t)\, e^*(\substack{\kappa \ b \\ \nu \ \alpha}) \exp[i\kappa \cdot r_0(\substack{l \\ 0})]. \tag{9}$$

where m_b is the mass of the b_{th} atom in the unit cell, u_α is the α component of the atomic displacement from equilibirum and $\dot{u}_\alpha$ is the α component of the atomic velocity and t is time t. The total energy of each vibrational mode is calculated from

$$E(\substack{\kappa \\ \nu}; t) = \frac{\omega(\substack{\kappa \\ \nu})^2}{2} q(\substack{\kappa \\ \nu}; t)^* \, q(\substack{\kappa \\ \nu}; t) + \frac{1}{2}\dot{q}(\substack{\kappa \\ \nu}; t)^* \, \dot{q}(\substack{\kappa \\ \nu}; t). \tag{10}$$

The vibrational mode lifetime is predicted using

$$\tau(\substack{\kappa \\ \nu}) = \int_0^{t^*} \frac{< E(\substack{\kappa \\ \nu}; t)\, E(\substack{\kappa \\ \nu}; 0) >}{< E(\substack{\kappa \\ \nu}; 0)\, E(\substack{\kappa \\ \nu}; 0) >} dt, \tag{11}$$

where the upper integration limit t^* is set to be much larger than the mode lifetime and the brackets indicate an ensemble average.[30] Equation (11) is derived by assuming that the energy autocorrelation follows an exponential decay.[60]

We perform the MD simulations using the fully disordered supercell and projecting onto the frequencies and eigenvectors from both the VC unit cell $[\omega(\substack{\kappa \\ \nu}), e(\substack{\kappa \ b \\ \nu \ \alpha})]$ and the Gamma supercell $[\omega(\substack{\kappa=0 \\ \nu}), e(\substack{\kappa=0 \ b \\ \nu \ \alpha})]$. The trajectories from these MD simulations are also used in the GK method calculations (Section IV). The MD simulations were ten times longer than the longest lifetime in the system, which was estimated from the VC-ALD predicted lifetimes. For LJ argon and SW silicon, data was collected for 2^{20} and 2^{22} time steps and the atomic

14

trajectories were sampled every 2^8 and 2^4 time steps, respectively. Ensemble averaging was performed using ten independent, initially-randomized velocity distributions.

For the normal modes of the lattice supercell, Eq. (11) is exact, but this expression becomes an approximation when using the VC normal modes to perform the mappings in Eqs. (8) and (9). Even for larger disorder ($c = 0.5$), where the energy autocorrelations deviate from an exponential decay, an effective lifetime can still be predicted using Eq. (11) (see Appendix A). The lifetimes predicted using VC-NMD and Gamma-NMD are shown in Figs. 4(a)-4(d) for the LJ argon crystal and all alloys at a temperature of 10 K. The range of frequencies for VC-NMD and Gamma-NMD differ slightly due to differences in the DOS (see Fig. 2). For a small interval of frequency, there is a wider range of predicted lifetimes for Gamma-NMD. This spread is because there is no symmetry-averaging of the mode properties, which is possible for the VC by considering the crystal lattice's irreducible Brillouin zone (BZ).[24]

The lifetimes predicted by both VC-NMD and Gamma-NMD show a ω^{-2} scaling at low frequency and a ω^{-4} scalings (for the alloys) and even faster for mid-range frequencies. These low- and mid-frequency scalings are predicted by the perturbative models used by the VC-ALD method (see Section III C 2). A constant lifetime is observed at the highest frequencies for both VC-NMD and Gamma-NMD except at $c = 0.5$ for VC-NMD. We are not aware of any theoretical prediction of this high-frequency behavior. The majority of the lifetimes predicted by both VC-NMD and Gamma-NMD are larger than the Ioffe-Regel (IR) limit,[62]

$$\tau = \frac{2\pi}{\omega}. \qquad (12)$$

The physical interpretation of the IR limit is a mode that scatters in a time equal to its oscillation period. Our results suggest that the IR limit is a good lower-limit for the lifetimes predicted by VC-NMD and Gamma-NMD for LJ argon (Fig. 4) and VC-NMD for SW silicon [see Fig. 8(a) in Section V].

Overall, good agreement is seen in the predicted lifetimes from VC-NMD and Gamma-NMD in both magnitude and trends. The use of the VC normal modes is an approximation that becomes worse as the concentration is increased (see Appendix A), but our results suggest that the effect is only pronounced at the highest frequencies. The only approximation associated with Gamma-NMD is the use of the harmonic lattice dynamics-predicted frequencies and eigenvectors to map the atomic trajectories from the fully anharmonic MD

15

simulations, ~~which~~ has been shown to be valid below temperatures of 40 K ~~for LJ argon~~.[60]
Based on the good agreement with Gamma-NMD, the lifetimes predicted by VC-NMD are used along with the VC-predicted group velocities to predict thermal conductivity in Section IV. For Gamma-NMD, there is no accepted way to predict the mode group velocities, so that the thermal conductivity can not be predicted using Eq. (1)

[handwritten annotations: "This assumption" inserted above "which"; "for LJ argon" written above; "one word" written below "can not"]
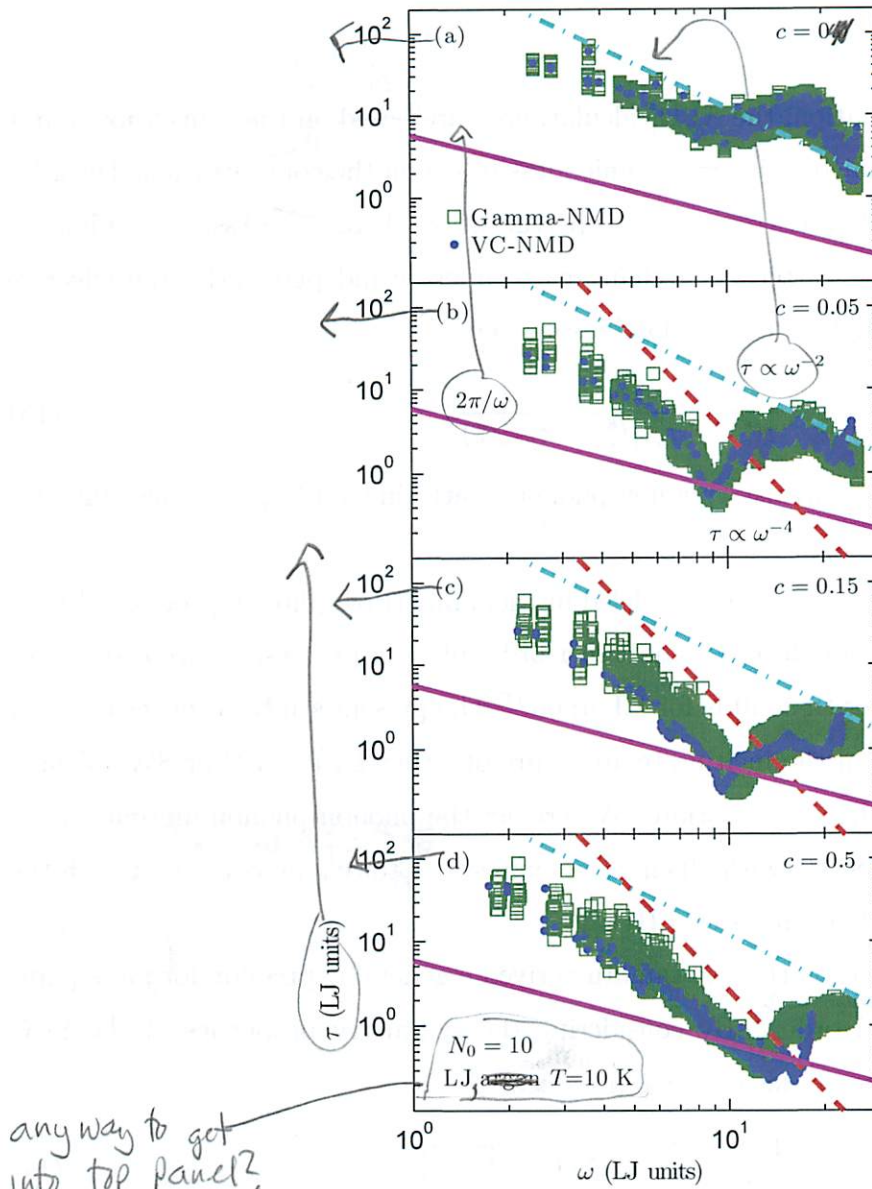
FIG. 4: Lifetimes predicted using VC-NMD and Gamma NMD from MD simulations of mass LJ alloys disordered ~~lattice supercells~~ (Section III C 1). Both ω^{-2} and ω^{-4} scalings can be observed at low frequencies, which are predicted by the peturbative models used for VC-ALD (Section III C 2). For both VC-NMD and Gamma NMD, most mode lifetimes are greater than the Ioffe-Regel limit $\tau = 2\pi/\omega$.[62] While there is more "noise" in the Gamma-NMD data (Section III C 1), the lifetime magnitudes and trends agree well, an important consideration when comparing VC-NMD and VC-ALD in Fig. 5 .

2. From VC-ALD

Under the VC approximation, the ALD calculations[60] are based on the conventional unit cells of LJ argon and SW silicon with the atomic mass based on the concentration. Disorder is not included explicitly but is treated using perturbation theory. Assuming phonon-phonon and phonon-defect scattering mechanisms to operate independently, the effective phonon lifetime can be found using the Matthiessen rule,[9]

$$\frac{1}{\tau\binom{\kappa}{\nu}} = \frac{1}{\tau_{p-p}\binom{\kappa}{\nu}} + \frac{1}{\tau_{p-d}\binom{\kappa}{\nu}},\tag{13}$$

where $\tau_{p-p}\binom{\kappa}{\nu}$ accounts for intrinsic phonon-phonon scattering and $\tau_{p-d}\binom{\kappa}{\nu}$ accounts for phonon-defect scattering.

Phonon-phonon scattering in ALD is modeled by including three-phonon processes.[13,15,60] It has been demonstrated that the effects of higher-order phonon processes[63] become important at temperatures greater than 40 K for LJ argon.[60] The present study is concerned with temperatures much less than the melting temperature of either LJ argon[45] or SW silicon[25] so that we believe ALD will be appropriate. We predict the phonon-phonon lifetimes using the method described in Ref. 60, with all classical expressions to remain consistent with the classical MD-based methods from Section III C 1.

Using harmonic perturbation theory, Tamura derived a general expression for mass point defect scattering to second order.[7] By considering the symmetry properties of the FCC lattices considered in this work, his expression reduces to

$$\frac{1}{\tau_{p-d}\binom{\kappa}{\nu}} = \frac{\pi}{2}g_2\omega^2\binom{\kappa}{\nu}\, DOS\left[\omega\binom{\kappa}{\nu}\right],\tag{14}$$

where

$$g_n = \sum_\mu c^\mu (1 - m^\mu/\bar{m}^\mu)^n.\tag{15}$$

Here, c^μ and m^μ are the concentration and mass of the μ-th species and $\bar{m}^\mu$ is the average mass. Bond disorder can be accounted for using a similar expression with an average atomic radius or suitable scattering cross-section.[33,34] For the binary LJ argon and SW silicon alloys considered here, there is one atom type in the unit cell with $\mu = i, j$, so that the alloying atom labeled by m_{1-c}^i can be considered to be an "isotope" of the atom labeled m_c^j. Tamura used this theory to predict the effect of defect scattering in isotopic germanium. The disordered

18

~~lifetimes are calcualted using Eqs (14) and (15).~~ To perform the calculation of Eq. (14), it is necessary to broaden the ~~discrete frequencies~~ *DOS* using using a Lorentzian function.[7] For all calculations, the Lorentzian was broadened using a value of $100\delta_{\omega,avg}$. ~~For the system sizes here,~~ the results do not differ significantly if this broadening value is varied manually or by increasing *the* system size ~~any~~.

[Handwritten top right: used $\delta\omega_{,avg}$ on p12 — why different here?]

[Handwritten left margin: Footnote 2 seems OK as main text]

The lifetimes predicted by VC-ALD for LJ argon at a concentration of 0.05 are plotted in Fig. 5(a). Also plotted are the lifetimes for the perfect system and from the VC-NMD predictions [Fig. 4(b)] at this concentration. At low frequencies, where the DOS is Debye-like [$D(\omega) \propto \omega^2$, Fig. 2], $\tau_{p-p}(\stackrel{\kappa}{\nu})$ scales as ω^{-2}, which is due to three-phonon scattering processes.[64] The scaling is also observed in the VC-NMD and Gamma-NMD *lifetimes*. Under the Debye-approximation the phonon scattering due to mass point-defects is predicted to scale as ω^{-4} and is observed in the VC-NMD, Gamma-NMD and VC-ALD predicted lifetimes in the mid-frequency range. VC-ALD does not predict the frequency-independent lifetimes at high frequency for LJ argon observed in VC-NMD and Gamma-NMD.

[Handwritten right margin: Integrate some of these comments in the previous section]

The Tamura theory was developed to predict the reduction of lifetimes in isotopic germanium, which is only perturbatively disordered ~~($\Delta m/\bar{m} \approx 0.05$~~ *(~5% variation in the atomic masses)*. The importance of higher-order interactions in the Tamura theory can be estimated by the disorder strength (i.e., g_n for $n > 2$).[7] For isotopically-disordered ~~Ge~~ *germanium, Tamura estimated that*, the higher-order contributions were ~~estimated to be~~ negligible ($g_3 \sim 10^{-7}$ and $g_4 \sim 10^{-7}$).[7] For *the* LJ argon *alloy*, and a concentration of 0.15 ~~in this work~~, $g_2 = 0.3018$, $g_3 = -0.3250$ and $g_4 = 0.4411$. It is possible that the neglect of the higher-order interactions in the Tamura theory is responsible for the discrepancy of the lifetimes predicted by VC-NMD and Gamma-NMD versus VC-ALD at high frequency. Evaluation of the higher-order interactions in the Tamura theory is of similar complexity to anharmonic phonon interactions for $n > 3$[60,63] and is beyond the scope of this work.

[Handwritten left margin: What is this g_2?]

[Handwritten bottom left: — Somewhere, discuss the use of Tamura theory by others for large mass ratios]

[Handwritten bottom center: In the LJ alloys, the two masses differ by a factor of three.]

[Handwritten bottom left: — Compare ALD, NMD for the perfect system (not just in caption) — lifetimes here, k in Section IV?]
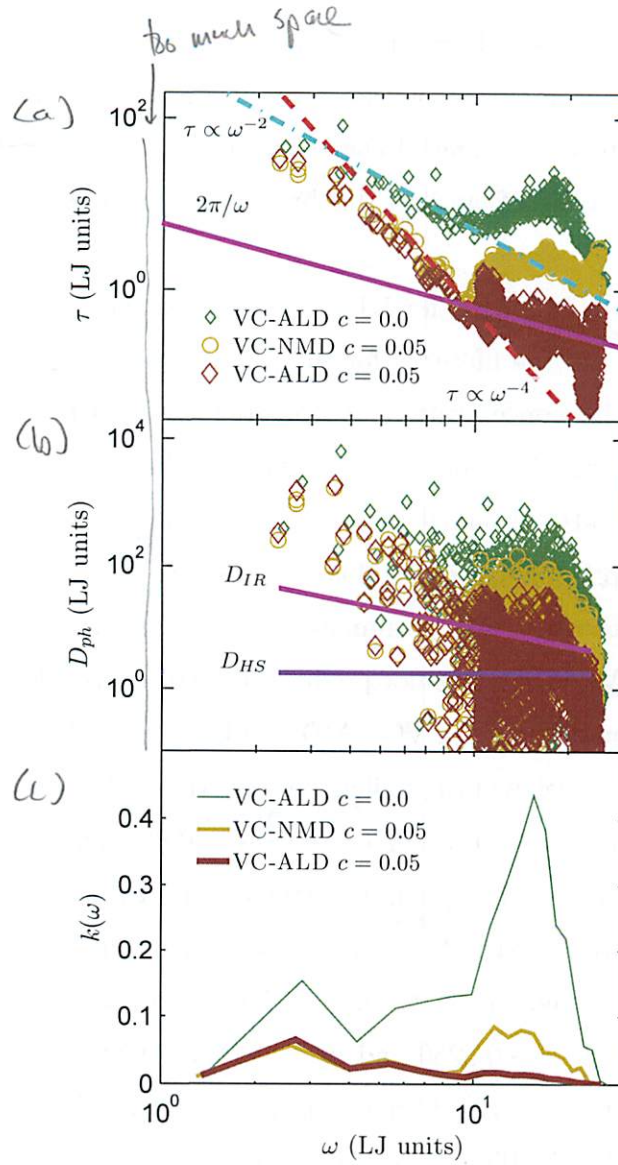
19

FIG. 5: (a) predicted lifetimes ~~for VC modes~~ using VC-NMD and VC-AlD for LJ argon ($T = 10$ K, $N_0 = 10$, and $c = 0.05$). The lifetimes predicted by VC-ALD and VC-NMD (not shown) agree at $c = 0.0$. (b) predicted VC mode thermal diffusivities, compared to the AF,HS limit. (c) the thermal conducitivty frequency spectrum, which is peaked at high frequency, in contrast to SW silicon (Fig 8).

[handwritten: This comment needs to be put in the main text and explained more— can you quantify?]

[handwritten: expand this caption]

pick one : diffusivity or Thermal diffusivity

D. Diffusivities

We now use the AF theory to provide a lower limit for the contribution to thermal conductivity of a given vibrational mode within the computational framework of the VC approximation. While studies have been performed on alloying the amorphous phase,[10] the AF theory has not been *previously* applied to disordered lattices. In the classical harmonic limit, *for a perfect crystal* where the specific heat is mode-independent, a mode's contribution to the thermal conductivity of a perfect crystal is determined by its thermal diffusivity,

need to be careful harmonic implies no phonon scattering

$$D_{ph,n}(\mathbf{\kappa}_{\nu}) = v_{g,n}^2(\mathbf{\kappa}_{\nu})\, \tau(\mathbf{\kappa}_{\nu}), \tag{16}$$

such that from Eq. (1)

$$k_{ph,n} = \sum_{\mathbf{\kappa}}\sum_{\nu} \frac{k_B}{V} D_{ph,n}(\mathbf{\kappa}_{\nu}). \tag{17}$$

The lower limit for phonon thermal diffusivity is zero since the group velocities can be zero (e.g., optical modes at the Brioullin zone center). Even for large disorder in the alloys, modes at low frequency have well-defined group velocities and lifetimes, which is demonstrated by the supercell structure factor peaks (see Fig. 3) and lifetimes predicted by VC-NMD, Gamma-NMD, and VC-ALD [see Figs. 4, 5(a)].

what is the purpose of this comment?

In a disordered system, modes can transport heat by harmonic coupling in the AF theory of diffusons [Eq. (2)].[31] In the HS limit,[1] the *thermal* diffusivity of each mode is

talk about D_{IR} here

$$D_{HS} = \frac{1}{3}v_s a, \tag{18}$$

footnote?

which leads to Eq. (3).[†] The Cahill-Pohl (CP) and AF HS limit differ by approximately *explain where the difference comes from* %20. The physical interpretation of Eq. (18) is that all vibrational modes transport heat *a transition is needed here!* at the sound speed and *have* scatter with a mean free path of the lattice spacing. For both *not italic* the VC-NMD and VC-ALD calculations, we approximate $v_{g,n}(\mathbf{\kappa}_{\nu})$ from the VC dispersion (Section III B) so that any differences in thermal diffusivity will come from the predicted lifetimes. As seen in Fig. 5(b) for the LJ argon alloy at a concentration of 0.05, VC-NMD and VC-ALD predict [from Eq. (16)] a significant number of modes with $D_{ph}(\mathbf{\kappa}_{\nu})$ *less than* D_{HS}.

Which component of v_g did you use?

While the HS model assumes a mode-independent thermal diffusivity, the AF theory is capable of predicting mode-specific thermal diffusivities.[10,32,65] Since the AF theory is harmonic, the thermal diffusivities typically diverge as the frequency approaches zero because these vibrations are long-wavelength plane waves that are weakly scattered by the

disorder.[66,67] The mode-specific thermal diffusivities of an LJ argon amorphous phase [§For a finite system, the AF theory requires a broadening in frequency to predict the mode-specific thermal diffusivities.[31] We use a Lorentzian broadening with a width of $\delta_{\omega,avg}$] are plotted in Fig. 6 along with the HS limit, Eq. (18), where the sound speed is estimated by

$$v_s = \frac{1}{3}v_{s,L} + \frac{2}{3}v_{s,T},$$ (19)

where $v_{s,L}$ and $v_{s,T}$ are the longitudinal and transverse sound speeds calculated from the elastic constants.[50] Except at the highest frequencies, the thermal diffusivity of all amorphous modes can be approximated using a mode-independent diffusivity of D_{HS}. Also plotted in Fig. 6 are the AF predicted thermal diffusivities for the explicitly-disordered LJ argon lattice supercell alloy at a concentration of 0.5. As expected, the AF theory predictions diverge at low frequency [¶For the disordered lattices studied in this work for $c \leq 0.15$, the predicted k_{AF} is strongly system-size dependent, indicating this diverging behavior. For LJ argon alloys at $c = 0.5$, the divergence with system size is small for the range of system size studied ($N_0 = 4$ to $N_0 = 12$, where $k_{AF}/k_{GK} = 0.93$ for $N_0 = 12$ because the finite system size limits the thermal diffusivities of the lowest frequencies.] The thermal diffusivity of all modes are larger than D_{HS} except at the highest frequencies, where they tend to zero as in the amorphous phase. This result supports the hypothesis that the lower-bound of the VC predicted phonon thermal diffusivity should be D_{HS}, which is further explored in Sections IV and V. Another possible lower-bound of thermal diffusivity based on the IR limit is

$$D_{IR} = \frac{2\pi}{3}\frac{v_s^2}{\omega}.$$ (20)

The CP model makes the same assumptions for group velocity (v_s) and lifetime ($2\pi/\omega$).[1] The lower bound D_{IR} is considered in Section IV.

22

E. Discussion

In this section, in anticipation of the thermal conductivity predictions in Section IV, we discuss two possible sources of error in the VC-predicted mode properties. For disordered systems, it is generally only possible to assign a unique lifetime and group velocity to vibrational modes in the low-frequency, propagating limit.[32,68] The thermal diffusivity is the fundamental transport property.[10,31,32] We believe that the VC-predicted group velocities, particluarly for $v_g(\mathcal{R}) \approx 0$, are an underprediction of the ~~representative~~ velocity scale ~~used~~ *[handwritten: required to evaluate]* ~~in Eq. (16) to calculate the thermal diffusivity of high-frequency modes in the disordered lattices.~~ This statement is supported by ~~considering~~ the AF theory ~~predicted mode~~ thermal diffusivities *[handwritten: plotted]* in Fig. 6, which are finite for the LJ alloy at a concentration of 0.5. While the thermal diffusivity from Eq. (16) can be zero because of the VC-predicted group velocities, this result is not consistent with the AF theory predictions. Predictions from model disordered systems demonstrate the existence of a plateau of the thermal diffusivity at high frequency, which is consistent with the minimum phonon mean-free path hyopthesis[69] used in most models of thermal transport in disordered materials.[1,70,71]

[Handwritten margin note: Important comment, but does not flow with the rest of the text, integrate!]

[Handwritten left margin: Vector or scalar? $\hat{v}^2$. Vector or scalar?]

The VC-NMD and Gamma-NMD predicted lifetimes are generally larger than the IR limit for LJ argon and its alloys (see Fig. 4). VC-ALD predicts essentially monotonically decreasing lifetimes with increasing frequency for the LJ argon alloys [Fig. 5(a)] with many falling below the IR limit. Because VC-NMD and VC-ALD use the same values for $v_g(\mathcal{R})$, the ~~phonon~~ mode diffusivities will therefore be underpredicted for VC-ALD compared to VC-NMD for the LJ argon alloys. ~~There are thus two underpredictions to consider when interpreting the thermal conductivity predictions in Section : (i) underprediction of the thermal diffusivity that results from using the VC group velocities for VC-NMD and VC-ALD, and (ii) the underprediction of the mode lifetimes for LJ argon alloys by the VC-ALD perturbative models.~~

[Handwritten margin note: repeating what was just said]

IV. THERMAL CONDUCTIVITY PREDICTIONS

The thermal conductivities of the LJ systems can now be predicted from Eq. (1) using the vibrational mode properties ~~predicted by the~~ *[handwritten: from]* VC-NMD and VC-ALD ~~methods~~. Given the discussion regarding the VC-predicted mode properties in Section III E, we also predict ther-

mal condudctivity using the equilibirum MD-based GK method, which is a top-down method that does not make any approximations about the nature of the normal modes. Thermal conductivities predicted by the GK method naturally capture all scattering meachanisms.[40,72,73] The heat current was computed every 10 time steps from the same atomic trajectories (positions and velocities) used for the VC-NMD and Gamma-NMD methods. In this study, the thermal conductivity is determined from the GK method by the maximum of the integral of the heat current autocorrelation function.

The thermal conductivities predicted by VC-NMD, VC-ALD, and GK are system size-dependent [i.e., $k = k(N_0)$] for all lattices except LJ argon at a concentration of 0. To predict a bulk thermal conductivity, k_0, a linear extrapolation procedure is used, whereby

$$\frac{k(N_0)}{k_0} = 1 - \frac{c_0}{N_0},$$ (21)

where c_0 is a constant.[16] For VC-NMD and VC-ALD, the validity of Eq. (21) requires that the low-frequency modes be dominated by phonon-phonon scattering (i.e., $\tau \propto \omega^{-2}$) and follow the Debye approximation with respect to the group velocity and DOS.[16,17] For the LJ argon alloys, this requirement is satisfied for modest system sizes (for $N_0 = 6$ to 12) so that both VC-NMD and VC-ALD predictions can be extrapolated to a bulk value.

Bulk thermal conductivity predictions for LJ argon alloys using VC-NMD, VC-ALD, and GK are tabulated in Table I and plotted in Fig. 7. Also plotted in Fig. 7 is the high-scatter thermal conductivity predicition, k_{HS} [Eq. (3)]. While agreement between the three methods is found for the perfect crystal, VC-NMD and VC-ALD underpredict the alloy thermal conductivities compared to GK. The underprediction is modest for VC-NMD (20% or less for all concentrations. The VC-ALD method underpredicts the thermal conductivity of the LJ argon alloys, where k_{VC-ALD} is 56% of k_{GK} at a concentration of 0.05.

In Section III D, we argued for the existence of a minimum mode thermal diffusivity, D_{HS} [Eq. (18)]. As shown in Fig. 5(b), the diffusivities of many high-frequency modes in the LJ alloys, predicted by both VC-NMD and VC-ALD, fall below this limit. Based on this observation, we propose that any thermal diffusivity below the limit be set to D_{HS} for thermal conducitivity prediction. The results of this adjustment, referred to as VC-NMD* and VC-ALD*, are plotted in Fig. 7 and included in Table I. The adjusted thermal conductivities predicted by VC-NMD* are within 10% of GK for all concentrations. Combined with D_{HS}, we believe that the VC-NMD predicted thermal diffusivities are good representations

25

for the explicitly disordered modes present in the MD simulation. Another possible adjustment, D_{IR} [Eq. (20)], results in an overprediction for LJ argon alloy at a concentraion of 0.05, $k_{VC-NMD^*_{IR}} = 0.94 \pm 0.09$ W/m-K, compared to GK, so we do not use this adjustment.

By applying the HS limit adjustment VC-ALD*, the thermal conductivities are brought into marginally better agreement, worst for a concentration of 0.05, where k_{VC-ALD^*} is 65% of k_{GK}. As seen in Fig. 5(b), the VC-ALD method fails to accurately predict the high-frequency mode thermal diffusivities for LJ argon alloys. Since the group velocities are the same for VC-NMD and VC-ALD, the underprediction of the high-frequency thermal diffusivities, and hence thermal conductivity, is due to the underpediction of the high-frequency mode lifetimes fro VC-ALD compared to VC-NMD, which we know are accurate values due to their agreement with Gamma-NMD. The thermal conductivity frequency spectrum is plotted in Fig. 5(c) and demonstrates that the thermal conductivity of LJ argon and its alloys are dominated by high-frequency modes. From this plot it can be seen that VC-ALD underpredicts the thermal conducitivity at high frequencies, consistent with lifetime underprediction by VC-ALD compared to VC-NMD.
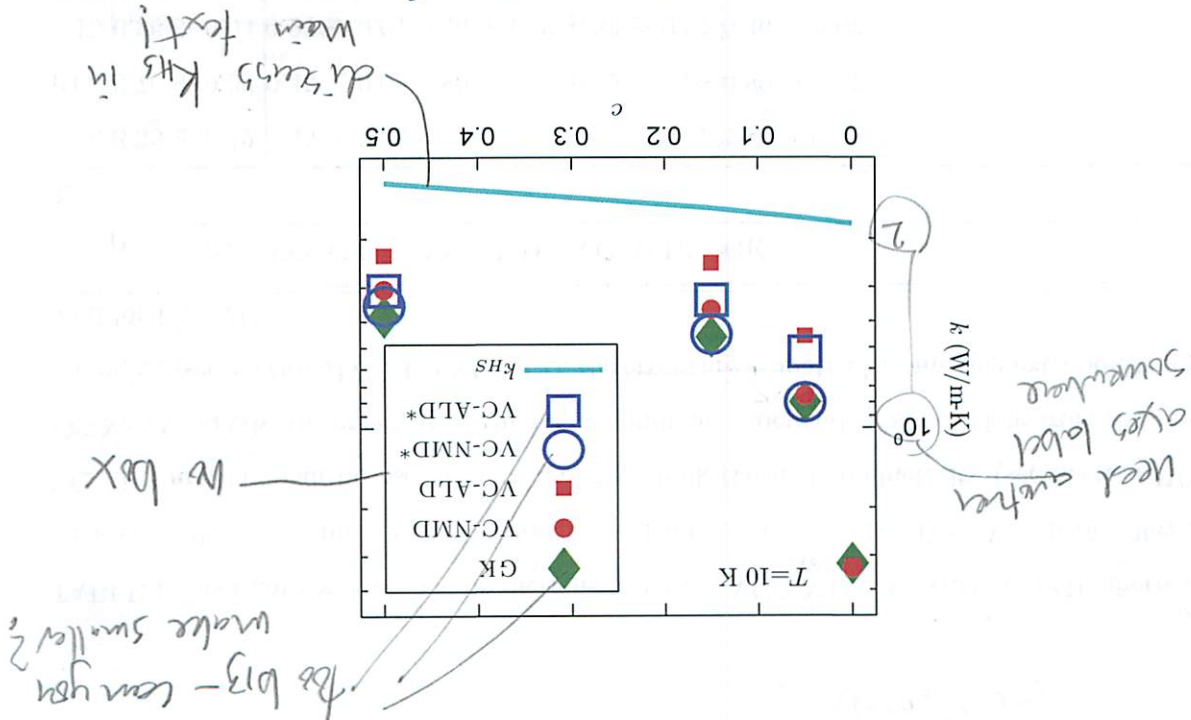
error → uncertainty

TABLE I: Thermal conductivity predictions using the VC-NMD, VC-ALD, and GK method. For LJ argon alloys, the bulk extrapolation is used for all *three* methods. For SW silicon alloys, only VC-ALD and GK can be used to extrapolate a bulk thermal conductivity (see Section IV). For VC-NMD and GK, the errors are estimated by omitting independent simulations from the ensemble averaging (see Section II C). For VC-ALD, the errors are *esimated* by omitting extrapolation points used for Eq. (21).

c	VC-NMD	VC-ALD	VC-NMD*	VC-ALD*	GK
LJ					
0.00	3.33 ± 0.12	3.45 ± 0.05			3.27 ± 0.09
0.05	0.76 ± 0.07	0.45 ± 0.02	0.80 ± 0.07	0.52 ± 0.05	0.80 ± 0.07
0.15	0.36 ± 0.04	0.24 ± 0.01	0.45 ± 0.05	0.33 ± 0.07	0.46 ± 0.07
0.50	0.31 ± 0.04	0.23 ± 0.01	0.35 ± 0.05	0.31 ± 0.07	0.38 ± 0.07
SW					
0.00		484 ± 21			517 ± 33
0.05	-----	23.5 ± 1.9		23.7 ± 1.9	20.1 ± 1.5
0.15		11.9 ± 0.9		12.0 ± 0.9	9.9 ± 0.9
0.50		11.1 ± 0.9		11.2 ± 0.9	9.3 ± 0.9

Columns need to be a bit wider

Why all this white space?

— you mix between two and three SF — what is most appropriate? two seems more reasonable given the uncertainties

V. SW SILICON

The failure of VC-ALD to predict the thermal conductivities of the LJ alloys is due to an underprediction of the high-frequency mode lifetimes, which dominate the thermal conducfivty [see Sections III D and IV, Figs. 5(a) and 5(c)]. To provide a contrast, we now predict the mode properties and thermal conductivity for bulk and alloyed SW silicon, where it is known that low-frequency modes dominate the thermal conductivity.[48,74] The lifetimes for the perfect crystal and an alloy concentration of 0.5 predicted by VC-NMD and VC-ALD are plotted in Fig. 8(a). The VC-NMD predicted lifetimes are generally larger than the IR limit for SW silicon alloys, similar to the VC-NMD predictions for the LJ argon alloys (Fig. 4). Unlike the LJ argon alloys, the VC-NMD and VC-ALD predicted lifetimes agree over most of the frequency spectrum, except at the highest frequencies, where VC-ALD underpredicts VC-NMD and falls below the IR limit. The high-frequency plateau of the VC-NMD predicted lifetimes for LJ argon (Fig. 4) is not seen for SW silicon.

As seen in Figs. 5(b) and 8(b), VC-NMD and VC-ALD both predict a significant number of modes with $D_{ph}(\vec{\varsigma})$ less than D_{HS} for both the LJ argon and SW silicon alloys, similar to the findings for the LJ alloys [Fig. 5(b)]. For SW silicon alloys, the thermal conductivity is dominated by low-frequency modes, so that large system sizes are needed to satsify the extrapaolation requirements and only GK and VC-ALD can be used, ($N_0 \leq 42$ in the present study, similar to the converged system sizes in [47]). This highlights the efficiency of the VC-ALD method, which is necessary when computationally expensive DFT calculations are used.[8,13,15,17,75,76] The SW silicon bulk thermal conductivity predictions for VC-ALD and GK are shown in Table I and plotted in Fig. 9. The thermal conductivities predicted for SW silicon alloys by VC-ALD and GK are in agreement within 20%, where VC-ALD overpredicts compared to GK. The overprediction of thermal conductivity by VC-ALD may be related to the role of disorder in the ALD calculation.[13,60] While Garg et al found an overprediction of VC-ALD compared to experiment by a factor of two, the overprediction we observe in this work for SW silicon alloys is not as drastic. The predicted thermal conductivities for the SW silicon alloys at all concentrations are over an order of magnitude larger than the HS predicition, k_{HS} [Eq. (3)]. As shown in Fig. 8(c), the thermal transport in SW silicon is dominated by low-frequency modes, such that the HS adjustment VC-ALD* vary by within only one percent compared to the unadjusted VC-ALD. As discussed in Section III C 2,
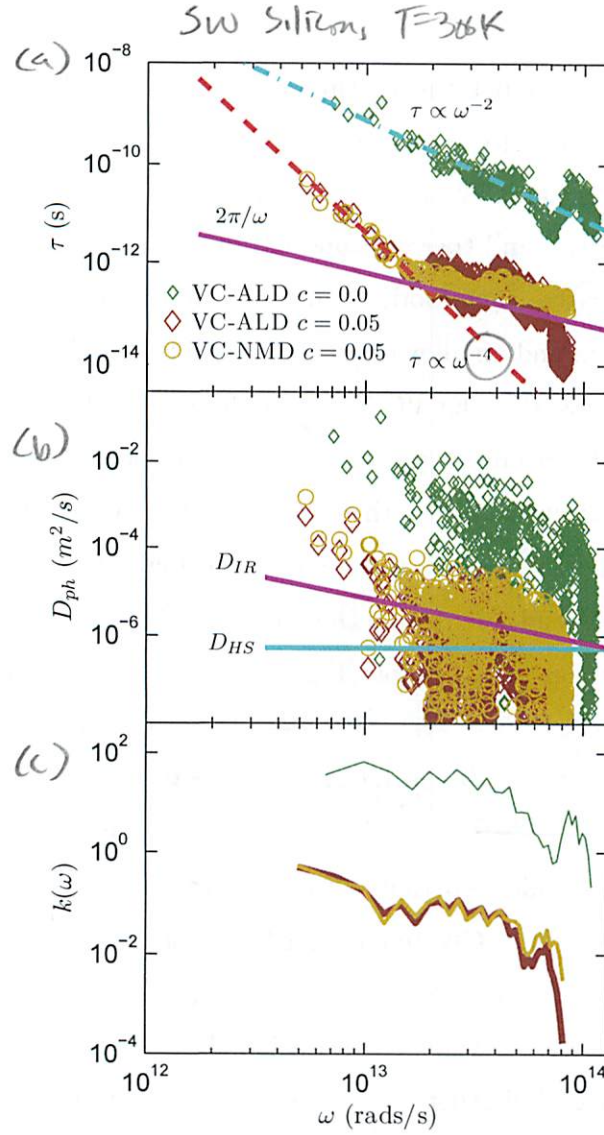
FIG. 8: (a) predicted lifetimes for VC modes using VC-NMD and VC-AlD for SW silicon. (b) predicted VC mode thermal diffusivities, compared to the AF,HS limit. (c) the thermal conducitivty frequency spectrum, which is peaked at low frequency, in contrast to LJ argon (Fig. 5).

While it is possible that higher-order interactions in the Tamura theory may be responsible for the discrepancy of the lifetimes predicted by VC-NMD and VC-ALD in SW silicon at the highest frequencies, but this discrepancy effect is unimportant to the overall thermal transport.

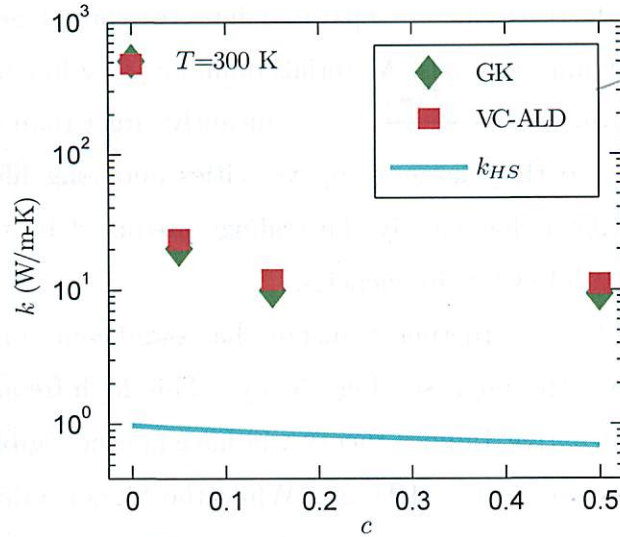*no box* (handwritten annotation)

FIG. 9: Thermal conductivity predictions for SW silicon alloys at a temperature of 300 K using the VC-NMD, VC-ALD, and GK methods. The high-scatter thermal conductivity prediciton k_{HS} (see Eq. (3)] is also plotted. The adjusted VC-ALD∗ is not shown since it differs by only one percent compared to VC-ALD. ~~The bulk thermal conductivity cannot be predicted using the VC-NMD method because computational demands limit the system sizes.~~

VI.   SUMMARY

In this study we investigated the use of the VC approximation for predicting the vibrational mode properties and thermal conductivity of LJ argon and SW silicon alloys by a detailed comparison of the NMD, VC-ALD, and GK methods. By using computationally- *inexpensive* ~~cheap~~ empirical potentials we self-consistently studied the effects of disorder both explicitly (Sections III A, III B, III C 1, III D, and V) and as a perturbation (Sections III C 2 and V). By spanning a range of disorder, ~~up to equal~~ the limits of the perturbative models were examined. A breakdown of the VC-ALD method was identified for LJ argon alloys by a comparison with the NMD method in Section III C 2 and a correction was suggested in Section III D. The mode properties and thermal conductivity of the SW silicon alloys were predicted and in Section V and provided a contrast to the LJ argon alloys, which have different thermal conducitivity spectra ~~than SW silicon alloys~~.

The results for the SW silicon and LJ argon alloys suggest that ~~thermal~~ modeling of *Thermal transport in*

ordered and disordered lattices can be separated into two broad groups: low-frequency dominated and full-spectrum materials. Materials dominated by low-frequency modes tend to have high thermal conductivities ~~which~~ that are significantly larger than the ~~high-scatter~~ HS limit ~~(Eq. (3))~~, which is due to their large group velocities and long lifetimes.[8,13,23,37–39,77,78] These low-frequency modes follow closely the scalings predicted by the perturbative VC-ALD models, which are valid at low-frequencies.

LJ argon is a material whose thermal transport has significant contribution from high-frequency modes, even for the bulk [see Fig. 5 (c)]. This high-frequency range is where we predict that the perturbative Tamura theory will have non-negligible contributions from higher-order interactions (see Section III C 2). While the higher-order interactions in the Tamura theory are also predicted to be non-negligible for SW silicon, this does not affect the thermal conductivity predictions significantly because high frequencies modes are unimportant to thermal transport. This also true for the thermal conductivity spectrum of SiGe alloys from theoretical predictions[12,13,23] and experimental measurements where the thermal conductivity exceeds the ~~high-scatter~~ HS limit by more than an order of magnitude at room temperature for all compositions.[1,38,39,78]

The VC-ALD method provides a computationally ~~cheap~~ inexpensive framework, which is essential ~~for expensive but experimentally accurate~~ when using ab initio methods for predicting thermal conductivity.[8,12–19] Based on our results, we believe the Tamura theory breaks down for mode thermal diffusivities predicted to be below the HS limit D_{HS} [Eq. (18)]. This may be true for the high-frequency modes of any disordered lattice, and the high-scatter limit D_{HS} should be considered whenever the perturbative VC-ALD method is used. Although the lower limit of thermal diffusivity is usually interpreted as a minimum mean free path,[1,69–71] we find that concept is not necessary for interpreting the results of this work. The fundamental quantity is the mode lifetime and the group velocity is an approximation, and expressed together as thermal diffusivity they can be interpreted in the presence of disorder.

Acknowledgments

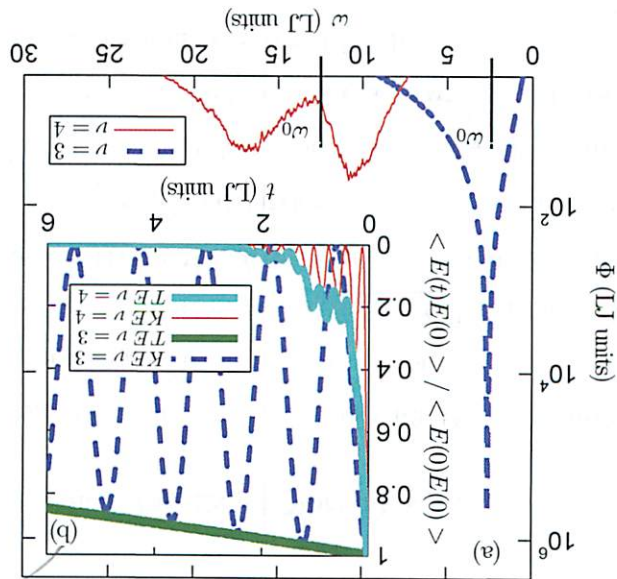Hasan, Craig Maloney, and Zhiting Tian for helpful discussions.

Appendix A: NMD using Non-Exact Normal Modes

For a normal mode of the lattice supercell used for the MD simulations (i.e., a Gamma mode), the total energy autocorrelation is an exponential function with a decay time $\tau(^\kappa_\nu)$ and the kinetic energy autocorrelation is a cosinusodial exponentially-damped oscillation with frequency $2\omega(^\kappa_\nu)$.(cite AHRT) When projecting onto the VC normal modes from MD simulations of the explicitly disordered lattice supercells, the energy autocorrelation fucntions do not always follow the simple functional forms, as shown in Figs. 10(a) and 10(b). By calculating the mode energy in the frequency-domain,[30] artifacts such as multiple peaks are observed for high concentrations, $c = 0.5$, Fig. 10.

These artifacts are not surprising given two considerations: (i) the MD simulations contain explicit disorder which influences the atomic trajectories, and (ii) the VC normal modes are not the exact normal modes of the explicitly-disordered lattice supercells. An effective lifetime can be predicted using Eq. (11) because the VC total mode energy autocorrelations still decay to zero in a finite time. This results is to be expected given that the atomic trajectories contain information about the lattice energy, which from general statistical physics principles will have exponential relaxation behavior in an equillibrium ensemble.[79–81]

FIG. 10: (a) The spectral energy density Φ of two modes (polarizations $v = 3, 4$ at wavevector [0.2 0 0]) calculated using VC-NMD for a mass disordered LJ FCC supercell ($N_0 = 8$ and $c = 0.5$). The VC dispersion-predicted peaks are labeled by ω_0. (b) the same mode's energy kinetic (KE) and total (TE) autocorrelation functions. Note the additional harmonic effects in the KE and TE autocorrelation functions for $v = 4$ which are due to the double peaks in Φ. A mode lifetime can be extracted unambiguously using the integral of the TE autocorrelation function (Section III C 1).

(handwritten annotations:)

don't use this term

This might then doesn't really make sense here

spectral energy here?

The lifes?

text4 caption shifts the versplot

?,

either make it a separate figure or refer to it as the inset (not its own figure)